Journal of Sound and Vibration 329 (2010) 2463–2476

Contents lists available at ScienceDirect

Journal of Sound and Vibration

journal homepage: www.elsevier.com/locate/jsvi

Detection of global and local parameter variations using nonlinear feedback auxiliary signals and system augmentation

Kiran D'Souza, Bogdan I. Epureanu *

Department of Mechanical Engineering, University of Michigan, 2350 Hayward Street, Ann Arbor, MI 48109-2125, USA

ARTICLE INFO

Article history:
Received 17 March 2009
Received in revised form
6 January 2010
Accepted 11 January 2010
Handling Editor: A.V. Metrikine
Available online 7 February 2010

ABSTRACT

Recently, system augmentation has been combined with nonlinear feedback auxiliary signals to provide sensitivity enhancement in both linear and nonlinear systems. Augmented systems are higher dimensional linear systems that follow trajectories of a nonlinear system one at a time. These augmented systems are subject to a specialized augmented forcing which enforces the augmented system to exactly reproduce the trajectory of the nonlinear system when projected onto the lower dimensional (physical) system. Augmented systems have additional benefits outside of handling nonlinear systems, which makes them more desirable than regular linear systems for sensitivity enhancing control. One of the key advantages of augmented systems is the complete control over the augmented degrees of freedom, and the additional sensor-type knowledge from the augmented variables. These sensing and actuation features are very useful when only few physical actuators and sensors can be placed. Such restrictions are common in most applications, and they severely limit the usefulness of traditional linear sensitivity enhancing feedback approaches. Another benefit of the augmentation is that the control exerted on the augmented degrees of freedom does not require any physical energy, rather it is just signal processing. In this work, these benefits are refined to improve the robustness of detection using sensitivity enhancement. Also, the benefits of system augmentation are explored by using few actuators and sensors. An optimization algorithm is employed not only to maximize the sensitivity of resonant frequencies to added mass at particular locations, but also to detect uniform changes in mass and stiffness. In addition to increased sensitivity for both global and local parameter changes, a study of increasing the sensitivity of local changes, while decreasing the sensitivity of global changes is conducted. Additionally, a methodology is presented to accurately extract augmented frequencies from displacement and forcing data corrupted by noise. Numerical simulations of cantilevered beams are used to validate the approach and discuss the effects of noise.

1. Introduction

Vibration-based identification of changes in structural parameters is currently used in a wide variety of technologies. In particular, two areas, sensing and damage detection, focus closely on identifying parameter variations such as mass and stiffness by exploiting variations in resonant frequencies. For example, recent sensing techniques for chemical and

* Corresponding author.
E-mail address: epureanu@umich.edu (B.I. Epureanu).

0022-460X/$ - see front matter © 2010 Elsevier Ltd. All rights reserved.
doi:10.1016/j.jsv.2010.01.011

biological detection as well as atomic force microscopes in tapping mode [1] use the vibration of micro-structures such as micro-beams [2] and micro-cantilevers [3–5].

Resonant frequencies are used not only for micro-scale systems but also for monitoring large-scale structures such as bridges, space and aircraft. Similar to sensing, vibration-based damage detection [6–8] uses changes in the systems modal properties to identify parameter variations indicative of damage. Some of these damage detection techniques use both mode shapes and natural frequencies, although measuring mode shapes is more sensitive to noise [9] than measuring frequencies, and requires more measurements.

Sensing and detection methods that use only the frequencies of the system (which herein are referred to as frequency-shift based methods [10]) have recently become of increasing interest. They have been developed because frequency extraction can be done robustly for both micro- and large-scale applications.

There are two central drawbacks to frequency-shift based methods. The first drawback is that only a limited number of frequencies can be measured accurately, which leads to an under-determined problem when solving for multiple different parameter variations (e.g. damage scenarios [11,12], or sensor outputs). To overcome this problem, in the context of damage detection, Cha and Gu [13] and Nalitolela et al. [14] proposed to extract additional modal frequencies by adding mass or stiffness to the structure. However, in practice, the physical addition of mass or stiffness is difficult to implement. This difficulty was overcome by Lew and Juang [15] by introducing virtual passive controllers. They used controllers to generate additional vibration frequencies in the closed loop system instead of attaching physical mass or stiffness elements to the structure. Additionally, Jiang et al. [16] has recently proposed a way to increase frequency measurements using tunable piezoelectric transducer circuitry.

The second drawback of frequency-shift based methods is that the sensitivity of the lowest frequencies to parameter variations is often quite low. Therefore, in sensing applications, the sensitivity of the sensors can be too low; and in damage detection applications, the lowest damage that can be identified is exceedingly large. For example, Swamidas and Chen [17] showed this in a finite element study of a cracked plate. In their study, a surface crack 40 percent the width of the plate and 70 percent through its depth had a maximum frequency shift of <0.7 percent. Adams et al. [18] demonstrated this low sensitivity experimentally using an aluminum bar under axial loading. They found less than a 1 percent change in the first three frequencies when they made a cut through 30 percent of the surface area of the beam near its center.

To overcome the insensitivity of the frequencies to parameter variations, Ray and Tian [19] proposed sensitivity enhancing feedback control. They applied closed loop vibration control for pole placement in smart structures with the objective of increasing the sensitivity of resonant frequencies to changes in the system. That method was demonstrated through numerical simulations of a cantilevered beam. Experimental validation of sensitivity enhancing feedback control was conducted by Ray et al. [20] on a cantilevered beam in bending. Ray and Marini [21] developed an optimization method to minimize the control effort while maximizing frequency sensitivity for a single fixed actuator location. Juang et al. [22] proposed an eigenstructure assignment technique that is useful in extending sensitivity enhancing control from single input to multi-input systems. Since in the multi-input case there are an infinite number of placement options for the modal frequencies, they chose the output feedback with the lowest control effort. They achieve this by using the open loop eigenvectors as the desired values of the closed loop eigenvectors, which leads to minimum control gains and minimum control effort. To address the limited frequency information drawback, Koh and Ray [23] proposed the use of multiple independent closed loop systems. Koh [24] also used sensitivity enhancing control for detecting damage nonlinearity due to the cyclic nature of crack breathing. Wang et al. [25] recently introduced a statistical pattern recognition method for damage detection in structures with sensitivity enhancement. Jiang et al. [26] developed an optimization algorithm for placement of frequencies and eigenvectors to maximize frequency sensitivity and minimize the control effort in the multi-input case. Jiang and Wang [27] applied the optimization algorithm for placement of frequencies and eigenvectors experimentally on a cantilevered beam. In their work, they also extracted the model of the system experimentally instead of using an analytical model.

One of the frontiers for the development of sensors and the advancement of damage detection technologies is tackling nonlinear systems. In these technologies, nonlinearities are often unavoidable during the regular vibration of the system, and hence, they have to be accounted for. Furthermore, they can be exploited for enhancing sensitivity. For example, recently sensitivity enhancing control has been proposed for nonlinear systems [28,29]. The nonlinear systems were handled by forming higher dimensional augmented linear systems [28–32], which are designed to follow a single trajectory of the nonlinear system. The idea of optimal augmentations has also been introduced by the authors [28]. The types of nonlinearities explored have included cubic spring nonlinearities [28–32] and Coulomb friction [31].

In this work, two cantilevered beams are explored using optimal system augmentations and nonlinear feedback auxiliary signals. The objective here is to build on the work of the authors [28,29] for the case where there are only limited measurements available and a single input actuator. In the first system, the motion of the structure, which must be fed back into the system using the control gain matrix, is known only at five locations. In the second system, the motion of the structure is known only at two locations. Linear approaches would allow for the placement of only two resonant frequencies in the first system and one in the second system. In contrast, the use of nonlinear feedback auxiliary signals allows the creation of several augmented variables, which increases the amount of measurement information, and in turn enables the placement of additional frequencies of the augmented system. Additionally, the simultaneous detection of global changes in the system (e.g. due to environmental changes in temperature or humidity) and local is explored. Also, the idea of sensitivity enhancement for parameters of interest combined with sensitivity reduction for parameters that are

not of interest (due to environmental or operational changes) is developed and explored. A methodology is also presented to accurately extract augmented frequencies from displacement and forcing data corrupted by noise. Various numerical simulations are included to demonstrate the proposed techniques, and to discuss the effects of random noise.

2. Methodology

In this section, the procedure for sensitivity enhancement using nonlinear feedback auxiliary signals in linear systems is presented. First, an overview of system augmentation with feedback auxiliary signals is provided. Second, the frequency-shift based detection procedure is outlined. Next, the optimization algorithm employed for controller design is discussed briefly. Finally, the augmented frequency extraction procedure is detailed.

2.1. System augmentation

In this section, a brief overview of system augmentation is provided. First, an example of a one degree of freedom system containing two nonlinearities is discussed. Then, the general form of the augmented equations are presented for a controlled system. Finally, an example of a simple controlled system is included. More details on system augmentation can be found in previous work by the authors [28–32].

Consider a mass connected to the ground by a linear, cubic and quintic spring. The equation of motion for this nonlinear system is given by

$$m\ddot{x}+kx+k_{n1}x^3+k_{n2}x^5=g(t), \tag{1}$$

where x is the position of the mass m, $g(t)$ is the external excitation, and k, $k_{n\,1}$, and $k_{n\,2}$ are the linear, cubic and quintic spring stiffnesses, respectively.

The fundamental idea behind the augmentation is that higher dimensional augmented linear systems can be designed to follow a single trajectory of a nonlinear system. For the nonlinear system in Eq. (1), a higher dimensional augmented linear system can be formed by adding an additional degree of freedom for each nonlinearity to obtain augmented equations of motion as

$$\begin{aligned} m\ddot{x}+kx+k_{n1}y_1+k_{n2}y_2&=g(t),\\ m_{a1}\ddot{y}_1+k_{c1}x+k_{a1}y_1&=h_1(t),\\ m_{a2}\ddot{y}_2+k_{c2}x+k_{a2}y_2&=h_2(t), \end{aligned} \tag{2}$$

where $y_1 = x^3$ and $y_2 = x^5$, with m_{ai}, k_{ai}, k_{ci}, $h_i(t)$, and y_i corresponding to the augmented mass, augmented stiffness, coupled stiffness, augmented forcing, and augmented variable, respectively.

Typically, the parameters k_{ci} are chosen to maintain the symmetry of the system ($k_{c\,1} = k_{n\,1}$ and $k_{c\,2} = k_{n\,2}$), m_{ai} are chosen similar to the mass at the degree of freedom they are coupled to ($m_{a\,1} = m_{a\,2} = m$), and k_{ai} are chosen to be low multiples of the nonlinear spring stiffness ($k_{a1}=\xi_1 k_{n1}$ and $k_{a2}=\xi_2 k_{n2}$ with constants ξ_1 and ξ_2 of values of about 2). However, one can choose these parameters to optimally suit their needs. An optimization of the augmentation for sensitivity enhancement has been established [28,29]. It uses the typical values of the augmentation as the starting point, and then optimizes the parameters k_{ci} and k_{ai} by finding the optimal control gains in the augmented equations. Additionally, a separate parameter is included in the optimization to adjust the augmented mass.

The augmented variables y_i can be computed directly from x ($y_1 = x^3$ and $y_2 = x^5$), and the augmented forcing $h_i(t)$ can be computed directly from the left hand side in Eq. (2). The specific form of the augmented forcing is a key feature in the augmentation because it ensures that, if the trajectory of the augmented linear system is projected onto the original (physical) space, it will follow the trajectory of the nonlinear system. Due to the required augmented forcing, the modal extraction technique used must be an input/output technique (as opposed to an output only approach).

There are several features of an augmented system that differ from a typical linear system and have to be considered when designing a controller for system interrogation. Consider the general equations of motion of an augmented system with a controller expressed as

$$\begin{bmatrix} \mathbf{M} & \mathbf{N}_I \\ \mathbf{N}_{CI} & \mathbf{N}_{AI} \end{bmatrix} \begin{bmatrix} \ddot{\mathbf{x}} \\ \ddot{\mathbf{y}} \end{bmatrix} + \begin{bmatrix} \mathbf{D} & \mathbf{N}_D \\ \mathbf{N}_{CD} & \mathbf{N}_{AD} \end{bmatrix} \begin{bmatrix} \dot{\mathbf{x}} \\ \dot{\mathbf{y}} \end{bmatrix} + \begin{bmatrix} \mathbf{K} & \mathbf{N}_S \\ \mathbf{N}_{CS} & \mathbf{N}_{AS} \end{bmatrix} \begin{bmatrix} \mathbf{x} \\ \mathbf{y} \end{bmatrix} + \mathbf{B} \begin{bmatrix} \mathbf{K}_{CL} & \mathbf{K}_{CN} \\ \mathbf{K}_{CLA} & \mathbf{K}_{CNA} \end{bmatrix} \begin{bmatrix} \mathbf{x} \\ \mathbf{y} \end{bmatrix} = \begin{bmatrix} \mathbf{g} \\ \mathbf{h} \end{bmatrix}, \tag{3}$$

where $\mathbf{M}$, $\mathbf{D}$ and $\mathbf{K}$ are the linear mass, damping and stiffness matrices; $\mathbf{N}_I$, $\mathbf{N}_D$, and $\mathbf{N}_S$ are nonlinear parameter matrices which contain terms such as the cubic and quintic stiffness terms; $\mathbf{N}_{CI}$, $\mathbf{N}_{CD}$, and $\mathbf{N}_{CS}$ are the coupled inertia, damping and stiffness matrices, which traditionally have been used to maintain the symmetry of the system; and $\mathbf{N}_{AI}$, $\mathbf{N}_{AD}$, and $\mathbf{N}_{AS}$ are the augmented parameter matrices, which contain terms such as m_{ai} and k_{ai}. $\mathbf{B}$ is the control input matrix, which has nonzero values in rows where there are input actuators that can excite the system.

An interesting advantage of augmented systems is that all the rows of the augmentation can have nonzero entries in **B** because they do not require any physical actuation. Also, the gain matrix $\mathbf{K}_C$ has been split into four parts in Eq. (3). The purely linear portion of the controller is given by $\mathbf{K}_{CL}$. The nonlinear portion of the controller is given by $\mathbf{K}_{CN}$. If a linear controller is desired $\mathbf{K}_{CN}$ must be set to zero. Finally, $\mathbf{K}_{CLA}$ and $\mathbf{K}_{CNA}$ are the augmented portions of the gain matrix. Note that no actual physical actuation is required in the augmented portion of the controller. Rather, the calculated actuation is used in the computation of the augmented forcing **h**.

Next, consider the augmented system discussed in Eq. (2) controlled by a single point actuator

$$\begin{aligned} m\ddot{x}+kx+k_{n1}y_1+k_{n2}y_2+K_{CL}x+K_{CN1}y_1+K_{CN2}y_2 &= g(t),\\ m_{a1}\ddot{y}_1+k_{c1}x+k_{a1}y_1+K_{CLA1}x+K_{CNA1}y_1 &= h_1(t),\\ m_{a2}\ddot{y}_2+k_{c2}x+k_{a2}y_2+K_{CLA2}x+K_{CNA2}y_2 &= h_2(t). \end{aligned} \tag{4}$$

The nonlinear actuation applied to the physical system is given by $K_{CN\ 1}y_1$ and $K_{CN\ 2}y_2$. Since augmented parameters (such as k_{ci} and k_{ai}) are chosen by the user, they can incorporate the augmented controller gains to obtain the following augmented equations of motion

$$\begin{aligned} m_{a1}\ddot{y}_1+k'_{c1}x+k'_{a1}y_1 &= h_1(t),\\ m_{a2}\ddot{y}_2+k'_{c2}x+k'_{a2}y_2 &= h_2(t), \end{aligned} \tag{5}$$

where $k'_{c1}=k_{c1}+K_{CLA1}$, $k'_{a1}=k_{a1}+K_{CNA1}$, $k'_{c2}=k_{c2}+K_{CLA2}$, and $k'_{a2}=k_{a2}+K_{CNA2}$.

The procedure for calculating the gain matrix $\mathbf{K}_C$ (containing linear and nonlinear control gains) consists of following an optimization algorithm previously established for augmented systems [28,29] and linear systems [26]. The procedure uses an eigenstructure assignment technique to place the eigenvectors and resonant frequencies of the augmented system, and is discussed in the subsequent sections.

2.2. Frequency-shift based detection method

In this section, the frequency-shift based detection method used in this work is outlined. The method is a first-order perturbation method, and has been used previously with sensitivity enhancing control [23,26,28]. Essentially, the idea is to relate the changes in the modal frequencies $\delta\boldsymbol{\omega}$ to the changes in certain parameters $\delta\mathbf{p}$ (e.g. stiffness, mass, damping parameters). Generally, the relationship between $\delta\mathbf{p}$ and $\delta\boldsymbol{\omega}$ is nonlinear. However, it can be linearized to a first-order perturbation form as

$$\delta\boldsymbol{\omega}=\mathbf{S}\delta\mathbf{p}, \tag{6}$$

where

$$\mathbf{S}=\begin{bmatrix} \frac{\partial\omega_1}{\partial p_1} & \frac{\partial\omega_1}{\partial p_2} & \cdots & \frac{\partial\omega_1}{\partial p_r}\\ \frac{\partial\omega_2}{\partial p_1} & \frac{\partial\omega_2}{\partial p_2} & \cdots & \frac{\partial\omega_2}{\partial p_r}\\ \vdots & \vdots & \ddots & \vdots\\ \frac{\partial\omega_q}{\partial p_1} & \frac{\partial\omega_q}{\partial p_2} & \cdots & \frac{\partial\omega_q}{\partial p_r} \end{bmatrix} \approx \begin{bmatrix} \frac{\Delta\omega_1}{\Delta p_1} & \frac{\Delta\omega_1}{\Delta p_2} & \cdots & \frac{\Delta\omega_1}{\Delta p_r}\\ \frac{\Delta\omega_2}{\Delta p_1} & \frac{\Delta\omega_2}{\Delta p_2} & \cdots & \frac{\Delta\omega_2}{\Delta p_r}\\ \vdots & \vdots & \ddots & \vdots\\ \frac{\Delta\omega_q}{\Delta p_1} & \frac{\Delta\omega_q}{\Delta p_2} & \cdots & \frac{\Delta\omega_q}{\Delta p_r} \end{bmatrix},$$

and the r index represents the number of parameters **p** that can change, the q index represents the number of measurable frequencies, and **S** is the sensitivity matrix. To determine the unknown changes in parameters from the known changes in frequencies, a pseudo-inverse of **S** in Eq. (6) can be used to yield

$$\delta\mathbf{p}=\mathbf{S}^{+}\delta\boldsymbol{\omega}. \tag{7}$$

When feedback interrogation is used, one sensitivity matrix **S** is obtained for each controller. For a controller of index i, the corresponding matrix is denoted by $\mathbf{S}^{ci}$. Also, the sensitivity matrix obtained when no controller is used (i.e. open loop) is denoted by $\mathbf{S}^{o}$.

The goal of sensitivity enhancement is to increase the entries in the closed loop sensitivity matrix $\mathbf{S}^{ci}$ with respect to the open loop sensitivity matrix $\mathbf{S}^{o}$. For a single closed loop system or for the open loop system, the solution of Eq. (7) is typically not very accurate because the number of changeable parameters r is likely greater than the number of measurable frequencies q, which results in an under-determined problem. Koh and Ray [23] overcame this problem by using multiple independent closed loop systems and unique combinations of actuator locations. Each closed loop system (of index i) corresponds to a unique sensitivity matrix $\mathbf{S}^{ci}$, which means that a complete closed loop sensitivity matrix can

be expressed as

$$\mathbf{S}^c = \begin{bmatrix} \mathbf{S}^{c1} \\ \mathbf{S}^{c2} \\ \vdots \\ \mathbf{S}^{cz} \end{bmatrix}, \tag{8}$$

where z corresponds to the number of unique controller configurations used. Therefore, if $z \cdot q > r$ then Eq. (7) becomes an over-determined set of equations for the unknowns $\delta\mathbf{p}$.

2.3. Optimization algorithm

The optimization algorithm used in this work is designed to determine the best control gains (linear and nonlinear) to enhance the sensitivity of the resonant frequencies of the augmented system to changes in particular structural parameters, while being subject to several constraints. The algorithm follows closely the work previously established for augmented systems [28,29] and linear systems [26], and uses an eigenstructure assignment technique to place the eigenvectors and resonant frequencies of the augmented system.

Two forms of the optimization algorithm are used in this work. The first was used in previous works [28,29] and has the form

$$J(\boldsymbol{\tau}) = C_1/SE + C_2 CE, \tag{9}$$

where J is the cost function that is minimized, $\boldsymbol{\tau}$ are the parameters being optimized, C_1 and C_2 are weighting coefficients, SE is the overall sensitivity enhancement that is maximized, and CE is the control effort that is minimized. The parameters $\boldsymbol{\tau}$ relate to the placement of the closed loop augmented eigenvalues and eigenvectors of the system, which can be used to determine the linear and nonlinear gain parameters (e.g. corresponding to the K_{CLi}, K_{CNi}, k_{ci} and k_{ai} terms from Section 2.1).

The control effort CE is defined as the absolute value of the maximum value in the controller gain matrix, not including the rows corresponding to the augmented degrees of freedom. The "control" of the rows corresponding to the augmented degrees of freedom does not require any physical actuation, just signal processing. This complete control authority with no physical actuation (for the augmented degrees of freedom) is one of the key advantages that nonlinear feedback auxiliary signals has over traditional sensitivity enhancing linear feedback.

The sensitivity enhancement SE is defined as the sum of the element by element ratio of the closed loop sensitivity matrices $\mathbf{S}^{ci}$ to the open loop sensitivity matrix $\mathbf{S}^o$ divided by the number of elements, i.e.

$$SE = \frac{\sum_{i=1}^{z}\sum_{j=1}^{q}\sum_{k=1}^{r}\left|\dfrac{\mathbf{S}^{ci}_{j,k}}{\mathbf{S}^{o}_{j,k}}\right|}{z \cdot q \cdot r}. \tag{10}$$

Eq. (7) is used to determine $\delta\mathbf{p}$ from $\delta\boldsymbol{\omega}$. Hence, in addition to purely sensitivity enhancement, it is important to also maximize the singular values (particularly the minimum singular value) of the sensitivity matrix $\mathbf{S}^c$ to increase the robustness of the method to noise.

The second optimization algorithm used in this work allows for simultaneous sensitivity enhancement for particular structural changes while also providing sensitivity reduction for other structural changes. Such combination of enhancement and reduction is needed in many applications where it is desirable to sense/detect variations in a parameter while being insensitive to other parameters (usually related to environmental or operational conditions). The corresponding cost function is given as

$$J(\boldsymbol{\tau}) = C_1/SE + C_2 CE + C_3 SR, \tag{11}$$

where C_3 is a weighting coefficient, and SR is a sensitivity reduction term.

Reducing the sensitivity for particular scenarios can be particularly useful for rejecting certain environmental or structural changes that are not of interest. For instance, a uniform change in stiffness that occurs in a beam due to temperature changes or fatigue may not be a change of interest, but can have a significant effect on the system. By reducing the sensitivity to these structural changes, the overall method becomes more robust to a larger array of environmental conditions. That is accomplished by minimizing SR (defined in a similar manner to the sensitivity enhancement term) given by the following expression

$$SR = \frac{\sum_{i=1}^{z}\sum_{j=1}^{q}\sum_{k=1}^{w}\left|\dfrac{\mathbf{Sr}^{ci}_{j,k}}{\mathbf{S}^{o'}_{j,k}}\right|}{z \cdot q \cdot w}, \tag{12}$$

where w is the number of parameters for which sensitivity is reduced, $\mathbf{Sr}^{ci}$ is the closed loop sensitivity matrix that is being minimized, and $\mathbf{S}^{o'}$ is the open loop sensitivity matrix for structural changes which are not of interest. Note that, in general, $\mathbf{S}^{o'}$ is distinct from $\mathbf{S}^o$ because $\mathbf{S}^{o'}$ includes only sensitivities to parameters that are not of interest.

Both optimization algorithms have certain built-in constraints. The first constraint requires that the physical linearized system be stable. However, the (fictitious) augmented system can be unstable. The linearized system must be stable for the healthy case and also for the maximum changes in each of its parameters. The second constraint enforces a linear relationship between each parameter change and the resonant frequencies. This constraint enables the use of the first-order frequency-shift based method explained in the previous section.

2.4. Frequency extraction for augmented systems

In this section, a procedure is presented for the extraction of augmented resonant frequencies from a system with few measurement locations and noisy data. The procedure is specially designed for augmented linear systems. However, with a few modifications, it can be used for standard linear systems also.

The first step in the procedure is to excite the system at a single frequency within the frequency range of interest. This frequency range corresponds to the (placed) frequencies of the closed loop augmented system. The response of the system and the physical excitation are stored. Multiple measurements can be performed (at the same frequency), and the measured response and excitation can be averaged at each phase of the dynamics. Hence, noise can be largely filtered out. That is particularly useful when the response of the system is periodic. Next, the harmonic excitation is repeated for additional frequencies until enough frequency information has been extracted from the system. Note that the ability to perform this noise filtering is a key consequence of the fact that the augmented system is linear.

The rest of the procedure deals with post processing and the actual extraction of the resonant frequencies. First, the augmented variables and the augmented forcing are constructed using the filtered data. The augmented variable $\mathbf{y}$ is computed directly from its nonlinear relation to $\mathbf{x}$, while $\ddot{\mathbf{y}}$ is calculated by finite differencing $\mathbf{y}$, and $\mathbf{h}$ is calculated directly from the left hand side of Eq. (3). Next, the full responses of the system ($\mathbf{x}$ and $\mathbf{y}$) and full forcing ($\mathbf{g}$ and $\mathbf{h}$) can be summed for all excitation frequencies to form a single (complex) excitation and response data set. The input ($\mathbf{g}$ and $\mathbf{h}$) and output ($\mathbf{x}$ and $\mathbf{y}$) can then be fed into DSPI [33], and the augmented frequencies can be extracted. Note that summing the response of the augmented systems over all frequencies is a key consequence of the fact that the augmented system is linear.

A specialized nonlinearity was designed for use in the nonlinear controller. It has the form $y = x^3 \exp(-x^2/C)$. A plot of this function for $C=1$ is shown in Fig. 1. The constant C is a scaling term that can be used to adjust the maximum amplitude and width of the nonlinearity. There are several key features that make this nonlinearity more desirable than other nonlinearities (such as cubic springs and Coulomb friction) that have previously been explored with system augmentation. First, this is a smooth nonlinearity, and its second derivative can be calculated accurately using finite differencing. Second, the peak amplitude of the variable y can be tailored to be close to the amplitude of the linear degrees of freedom (by choosing an adequate value for C). Finally, the last key feature is that the nonlinear response tends to zero for large amplitudes in the system. This feature is important in making sure that the system response remains bounded during its interrogation. Since the nonlinearity exponentially tends to zero at large x, and since the open loop (physical) linear system is stable, the closed loop system returns toward the origin when the response becomes large. Although other nonlinearities can be used with nonlinear feedback auxiliary signals, the nonlinearity used is particularly effective because of the three key features explained above.

3. Numerical results

In this section, numerical simulations were performed on two cantilevered beam systems. First, the system shown in Fig. 2 was investigated. In particular, the frequency extraction method was investigated to determine how sensitive to

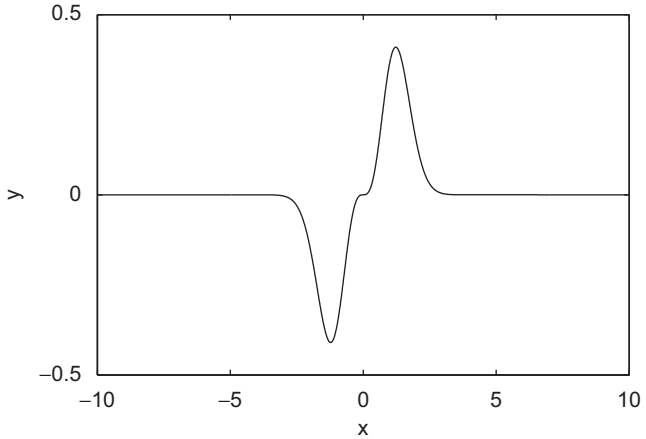

Fig. 1. Nonlinearity used in the nonlinear controllers.

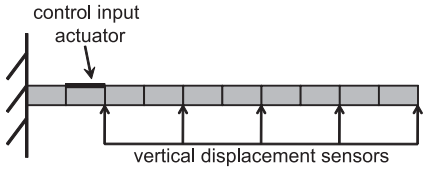

Fig. 2. Linear beam excited by one piezoelectric patch using nonlinear feedback auxiliary signals from five sensors.

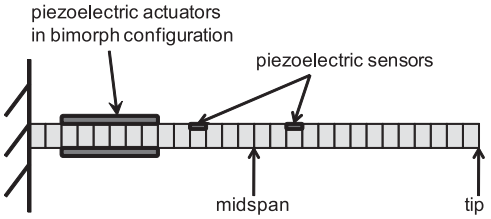

Fig. 3. Linear beam excited by piezo-actuators using nonlinear feedback auxiliary signals and two piezo-sensors.

noise the extraction process is. Also, a comparison of nonlinear feedback auxiliary signals, linear feedback, and an uncontrolled system was conducted under various conditions. Next, the system in Fig. 3 was investigated. Due to the reduced measurements, linear feedback was not feasible and nonlinear feedback auxiliary signals were directly compared with the open loop system. In particular, two sets of nonlinear feedback auxiliary signals were designed (1) to detect variations in both global and local parameters, and (2) to detect local changes while being insensitive to global changes. The local changes are variations of the mass of the beam in the vicinity of its tip and midspan (which correspond to sensing scenarios). The global changes are proportional variations in the entire mass or stiffness of the physical system. The uniform change in mass scenario could result from a change in humidity, while the uniform change in stiffness scenario could result from a change in temperature. The ability to distinguish the effects of humidity and temperature from the changes due to local additions of mass is critical for practical uses of this method for sensing and damage detection.

3.1. Case 1

To demonstrate the augmented frequency extraction and the benefits of nonlinear feedback auxiliary signals over linear feedback, a numerical investigation was performed on a linear cantilevered beam shown in Fig. 2. The properties of the system are the same as the system investigated by Jiang et al. [26]. The density and Young's modulus of the beam are $2410\,\mathrm{kg/m^3}$ and $6.6\times10^{10}\,\mathrm{N/m^2}$, respectively. The length, thickness, and width of the beam are 400, 3.4, and 26 mm. The density and Young's modulus of the piezoelectric material are $7600\,\mathrm{kg/m^3}$ and $5.9\times10^{10}\,\mathrm{N/m^2}$, respectively. The length, thickness, and width of the piezoelectric patch are 40, 0.3, and 20 mm. The piezoelectric constant is $d_{31}=\text{-}276\times10^{-12}\,\mathrm{m/V}$. The beam was discretized into 10 elements with the control and forcing input to the system applied through a moment induced by the piezoelectric patch on the second element of the beam. A light proportional damping of the form $\alpha\mathbf{M}+\beta\mathbf{K}$ was also added to the beam, where $\alpha=10^2$ and $\beta=10^{-5}$. Five position measurements (out of a possible 20 degrees of freedom for the system model) were taken along the beam, as indicated in Fig. 2.

In addition to the five physical measurements, five augmented variables were created for the system. The augmented variables are $y_i = x_i^3 \exp(-x_i^2/C)$, where x_i are the five measured signals. Only these nonlinearities are used in the controller. The augmented system was created by generating $\mathbf{M}$, $\mathbf{K}$, $\mathbf{N}_I$, $\mathbf{N}_S$, $\mathbf{N}_{AI}$, $\mathbf{N}_{AD}$, $\mathbf{N}_{AS}$ and $\mathbf{N}_{CS}$ as discussed in the system augmentation section. The augmented matrices and control gains were optimized using the "fmincon" function in MATLAB [34].

In general, the user has complete control over the five augmented degrees of freedom corresponding to the five augmented variables. Hence, multiple independent closed loop configurations are possible (even though there is only one physical controller). In this work, the only controller configuration that was used corresponds to control at the physical degrees of freedom affected by the piezoelectric patch and the five augmented degrees of freedom.

The first five resonant frequencies of the system were optimally placed to maximize the sensitivity and linear independence for four scenarios. The first scenario corresponds to added mass at the tip of the beam. The second scenario corresponds to added mass at the midspan of the beam. The third scenario corresponds to a uniform change in mass of the physical system (e.g. a change in humidity of the environment). The fourth scenario corresponds to a uniform change in stiffness of the physical system (e.g. a change in temperature of the environment).

Two controllers were designed to enhance the sensitivity of the resonant frequencies. The first one was based on traditional linear feedback. Due to the fact that only two frequencies could be placed, this controller was created to detect only the local changes in mass at the tip and midspan (and was not designed to detect uniform changes in the mass

Table 1
First seven eigenvalues of a baseline (nominal) closed loop system for no noise and for a case with a Gaussian distributed noise with zero mean and a standard deviation of 0.5 percent of the response (and excitation) of the system.

Exact augmented eigenvalues	Augmented eigenvalues extracted by DSPI (no noise)	Average augmented eigenvalues extracted by DSPI (noisy measurements)	Standard deviation of augmented frequencies extracted by DSPI
−50.449 + 320.8487i	−50.4304 + 320.845i	−56.0636 + 320.6479i	2.4056
−51.1395 + 1887.875i	−51.2038 + 1887.8741i	−51.7111 + 1887.4735i	0.3035
−59.0027 + 2031.5986i	−58.9349 + 2031.5773i	−60.7222 + 2033.4844i	0.625
−135.8709 + 3658.8146i	−135.7516 + 3658.7827i	−135.8077 + 3659.1526i	0.4331
−260.9331 + 5581.6613i	−261.0341 + 5581.6112i	−260.8428 + 5581.6889i	0.558
−510.741 + 9425.9538i	−510.6796 + 9426.1458i	−511.3594 + 9426.7778i	1.1731
−959.1626 + 13960.3522i	−958.6539 + 13960.5427i	−959.5121 + 13960.5772i	3.216

Table 2
First seven eigenvalues of a baseline (nominal) closed loop system for no noise and for a case with a Gaussian distributed noise with zero mean and a standard deviation of 1.0 percent of the response (and excitation) of the system.

Exact augmented eigenvalues	Augmented eigenvalues extracted by DSPI (no noise)	Average augmented eigenvalues extracted by DSPI (noisy measurements)	Standard deviation of augmented frequencies extracted by DSPI
−50.449 + 320.8487i	−50.4304 + 320.845i	−61.9684 + 322.1665i	3.1866
−51.1395 + 1887.875i	−51.2038 + 1887.8741i	−52.4337 + 1886.7524i	0.3067
−59.0027 + 2031.5986i	−58.9349 + 2031.5773i	−66.6076 + 2036.5810i	0.9933
−135.8709 + 3658.8146i	−135.7516 + 3658.7827i	−135.7568 + 3658.6498i	0.4168
−260.9331 + 5581.6613i	−261.0341 + 5581.6112i	−260.7681 + 5582.1474i	0.5944
−510.741 + 9425.9538i	−510.6796 + 9426.1458i	−510.9183 + 9426.7582i	1.6176
−959.1626 + 13960.3522i	−958.6539 + 13960.5427i	−962.2222 + 13952.8001i	5.7744

and stiffness). The second controller is based on nonlinear feedback auxiliary signals. Due to the added control and sensing, five frequencies could be placed. Hence, both the local and the global variations can be detected.

To demonstrate the frequency extraction method, the eigenvalues of the healthy augmented system were obtained using DSPI for the case of zero measurement noise and for the case of measurement noise (with a Gaussian distribution, zero mean, and a standard deviation of 0.5 percent of the response of the system). The results are presented in Table 1. The first column consists of the first seven exact eigenvalues. The second column consists of the eigenvalues extracted by DSPI for the noise-free case. The third column contains the average values of the eigenvalues obtained from 100 separate numerical simulations for the noisy case. The fourth (and last) column consists of the standard deviations obtained for the identified frequencies. Comparing the first two columns one may note that DSPI can very accurately extract the augmented eigenvalues of the system for zero noise. In the presence of noise, the method still works quite well with the average value very close to the exact eigenvalue (with small deviations).

To observe how the extraction is affected by a larger amount of noise, the results for a noise with a Gaussian distribution having zero mean and a standard deviation of 1 percent of the response of the system are presented in Table 2. The columns of Table 2 are laid out in the same manner as in Table 1. An interesting observation from Tables 1 and 2 is that the lowest extracted augmented frequency has the second largest standard deviation. Although typically higher resonant frequencies are more sensitive to noise effects, in this case it was observed that the response of the system at the lowest frequency was smaller than that of the other (low) frequencies. As a result, when noise is added into the measurements, the lowest resonant frequency has a higher sensitivity to noise.

For the following results, the exact frequencies were calculated for the system, and a noise with a Gaussian distribution having zero mean was added to the *eigenvalues* of the system. The standard deviation for the noise distribution was approximately equal to the standard deviations for the frequencies given in Table 1.

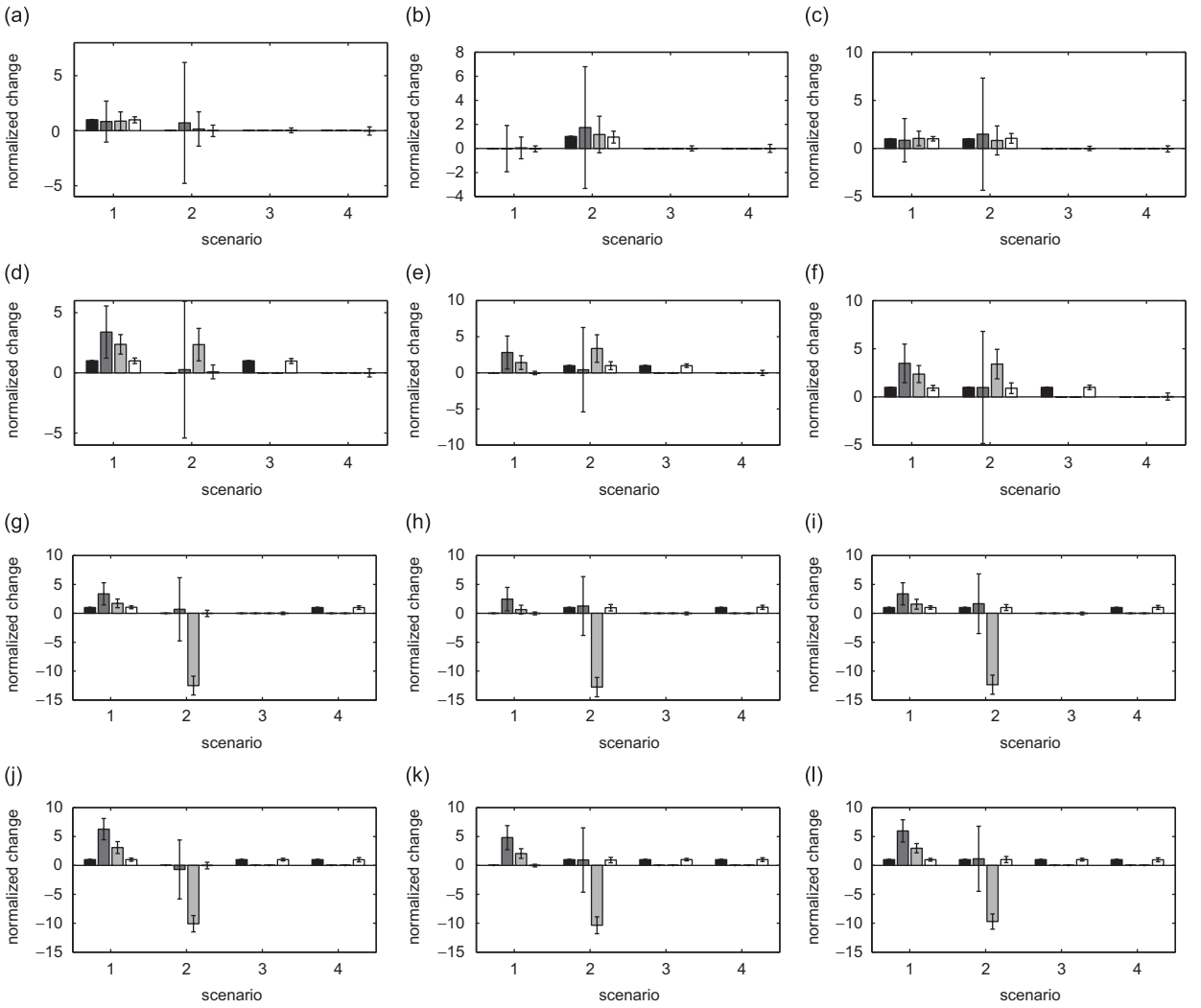

Fig. 4. Sensed mass and/or stiffness: (i) by the open loop system (dark grey), (ii) by a system with linear feedback unable to detect uniform mass and stiffness changes (light grey), (iii) by a system with nonlinear feedback auxiliary signals which is able to detect uniform mass and stiffness changes (white), and (iv) the exact changes (black). Scenario 1 represents changes in mass at the tip. Scenario 2 represents changes in mass at the midspan. Scenario 3 represents a uniform change in mass. Scenario 4 represents a uniform change in stiffness. (a) Scenario 1, (b) Scenario 2, (c) Scenarios 1 and 2, (d) Scenarios 1 and 3, (e) Scenarios 2 and 3, (f) Scenarios 1, 2, 3, (g) Scenarios 1 and 4, (h) Scenarios 2 and 4, (i) Scenarios 1, 2, 4, (j) Scenarios 1, 3, 4, (k) Scenarios 2, 3, 4, and (l) Scenarios 1–4.

The results in Fig. 4 show the changes predicted for a variety of different cases. The plots on the left correspond to a case where a mass of 0.1 percent of the beam is placed at the tip of the beam. The plots in the center correspond to the case where a mass of 0.1 percent of the beam is placed at the midspan of the beam. The plots on the right correspond to the case where there are masses (each of 0.1 percent of the beam) placed at both the tip and at the midspan of the beam. The top row of plots corresponds to a case where there are no uniform mass or stiffness changes. The second row of plots corresponds to the case where there is a uniform mass change, while the third row of plots corresponds to a uniform stiffness change. The fourth (and final) row of plots corresponds to a uniform change in both mass and stiffness. There are four bars plotted for each plot. The first bar is the exact change in the system. The rest of the bars have standard deviation error bars for the noisy cases. The second bar is the value predicted by an open loop system. The sensitivity matrix of the open loop system would be rank deficient if it was taking into account uniform mass and stiffness changes. Therefore, a sensitivity matrix based solely on added mass at the tip and midspan was created for the open loop case (in the same way as done for linear feedback). The third bar is the change predicted when enhancing sensitivity using traditional linear feedback (which can only detect the local changes due to the limited sensing and control authority). The fourth (and final) bar is the change predicted when enhancing sensitivity through nonlinear feedback auxiliary signals. For the case when there are no uniform changes in mass or stiffness, the linear feedback gives a significant improvement over the uncontrolled system, and nonlinear feedback auxiliary signals provides an even greater improvement. When there are

uniform changes in mass and/or stiffness, both the uncontrolled and linear feedback perform very poorly because they are not able to distinguish the additional (global) changes from the local changes, while the approach based on nonlinear feedback auxiliary signals is able to detect simultaneously all of the changes in parameters.

3.2. Case 2

To demonstrate several of the additional advantages of nonlinear feedback auxiliary signals over linear feedback, and in particular their ability to enhance or reduce global changes, numerical simulations were performed on a linear cantilevered beam shown in Fig. 3. The beam is made of aluminum with a density and Young's modulus of 2660 kg/m^3 and 68.9 GPa, respectively. The length, width, and thickness of the beam are 280 mm, 15 mm, and 1.27 mm, respectively. The piezo-actuator patches are placed in a bimorph configuration 20 mm from the root. The density, Young's modulus, and piezoelectric constant are 7800 kg/m^3, 62 GPa, and $d_{31} = -300 \times 10^{-12}$ m/V, respectively. The length, width, and thickness of each piezoelectric patch is 60, 15, and 1 mm, respectively. The beam was discretized into 28 elements with two degrees of freedom per node. The linear beam model had a total of 56 degrees of freedom. The piezo-sensors placed 100 and 160 mm from the root of the beam were assumed to have a negligible impact on the properties of the system. The excitation of the beam by the piezo-actuators was modeled as an induced moment due to an applied voltage. The sensor information used as feedback was a voltage from each sensor that was related to the curvature of the beam, which in turn can be related to the rate of change in the slope of the beam at the location of the sensor. In addition to the two physical measurements, two augmented variables were created for the system.

In general, the user has complete control over the two augmented degrees of freedom corresponding to the two augmented variables. Hence, multiple independent closed loop controllers are possible (even though there is only one physical controller). Hence, note that in this work the only controller configuration that was used corresponds to control applied at the physical degrees of freedom affected by the piezo-actuator and the two augmented degrees of freedom.

3.2.1. Detecting local and global changes

The first set of results consist of designing nonlinear feedback auxiliary signals for sensitivity enhancement for four different scenarios. The four scenarios are the same as the ones in the previous section where the first two scenarios correspond to local changes in the mass of the system, and the last two scenarios correspond to global mass and stiffness changes.

Due to the limited sensor information and control authority in this challenging example, only the first two resonant frequencies of the system could be placed using nonlinear feedback auxiliary signals. This is an *improvement* over purely linear feedback which would only be able to place a single frequency. Since there are four scenarios and only two frequencies, the optimization is carried out twice to obtain two distinct sets of nonlinear feedback auxiliary signals. This ability to extract two distinct sets of nonlinear feedback auxiliary signals for the same controller configuration is an additional benefit of this approach over traditional linear feedback. These nonlinear feedback auxiliary signals were optimized for both sensitivity enhancement and linear independence between the nonlinear feedback auxiliary signals such that the global sensitivity matrix is full rank.

For the following results, the exact frequencies were calculated for the system, and a zero mean white noise was added to the eigenvalues of the system. The noise level was approximately ± 0.2 percent of the lowest frequency. This noise level is less than the noise used in the previous case because this detection scenario is much more challenging since only two sensors are being used. The results in Fig. 5 show the changes predicted for a variety of different cases. The plots are laid out in the same manner as in Fig. 4. In each plot, there are three bars shown, where the first bar is the exact change in the system. The other two bars are shown together with standard deviations (for the noisy cases). The second bar is the average value predicted by the open loop linear system. The sensitivity matrix of the open loop system would be rank deficient if it were taking into account uniform mass and stiffness changes (and that would lead to inaccurate results). Therefore, a sensitivity matrix based solely on added mass at the tip and midspan was created for the open loop results. The third bar is the average change predicted by nonlinear feedback auxiliary signals. The improvement of the nonlinear feedback auxiliary signals over the open loop predictions are significant even for this limited case of one controller and two sensors. Note especially the reduction in noise effects.

3.2.2. Detecting local changes and ignoring global changes

The next group of results consist of designing a new set of feedback auxiliary signals that are sensitive to local changes in the mass placed at the tip and midspan, but insensitive to global (uniform) changes in the mass and stiffness.

Similar to the results above, two resonant frequencies of the system were placed using nonlinear feedback auxiliary signals, but since there are only two scenarios being detected, only one set of nonlinear feedback auxiliary signals was used. The plots in Fig. 6 are laid out in a similar manner to Fig. 5. However, only the local changes are plotted (scenarios 1 and 2) since the effects of the global changes are not of interest (and have been minimized). For the following results, the exact frequencies were calculated for the system, and a zero mean white noise was added to the eigenvalues of the system. The noise was approximately ± 0.3 percent of the lowest frequency. Note that the noise used in this case is larger than in the previous case. Nonetheless, the standard deviation error bars are smaller for the nonlinear feedback auxiliary signals

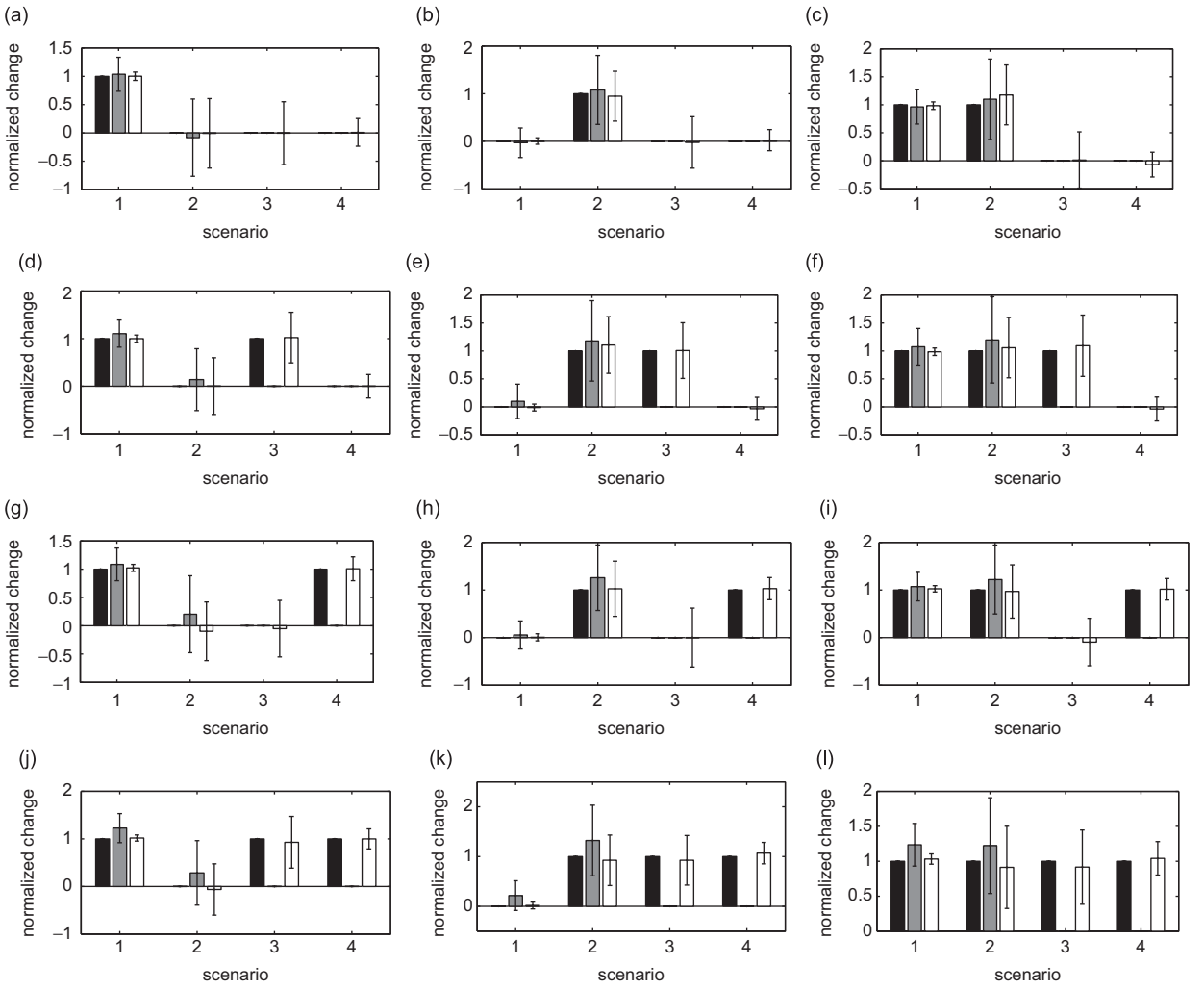

Fig. 5. Sensed mass and/or stiffness: (i) by the open loop system (grey), (ii) by a closed loop system designed to detect uniform mass and stiffness changes using nonlinear feedback auxiliary signals (white), and (iii) the exact changes (black). Scenario 1 represents changes in mass at the tip. Scenario 2 represents changes in mass at the midspan. Scenario 3 represents a uniform change in mass. Scenario 4 represents a uniform change in stiffness. (a) Scenario 1, (b) Scenario 2, (c) Scenarios 1 and 2, (d) Scenarios 1 and 3, (e) Scenarios 2 and 3, (f) Scenarios 1, 2, 3, (g) Scenario 1 and 4, (h) Scenarios 2 and 4, (i) Scenarios 1, 2, 4, (j) Scenarios 1, 3, 4, (k) Scenarios 2, 3, 4, and (l) Scenarios 1–4.

than in the previous case, highlighting the better performance of the nonlinear approach. The system using nonlinear feedback auxiliary signals shows improvement over the open loop predictions in this case for both the average values as well as the effects of noise. These plots show that lowering the influence of unwanted environmental changes or operational conditions on frequency shifts can be achieved through sensitivity reduction (in combination with sensitivity enhancement for the desired parameters).

The final set of results are based on setting up two distinct sets of nonlinear feedback auxiliary signals, which create a sensitivity matrix, which is overdetermined with respect to the two scenarios of interest. The results are shown in Fig. 7, where the plots are laid out in the same manner as in Fig. 6. A zero mean white noise was added to the eigenvalues of the system. The noise was approximately ± 0.5 percent of the lowest frequency. Note that this noise level is significantly greater than the previous two cases. Even with the greater noise, the error bars on the nonlinear feedback auxiliary signals are comparable to the previous cases, and overall there is an improved prediction of the changes in mass. These results show that the use of an overdetermined sensitivity matrix (which allows for variation of the global parameters in an unobserved subspace) improves the local detection of mass variations.

4. Conclusions and discussion

A novel approach for sensitivity enhancement for linear and nonlinear systems via optimal augmentations and nonlinear feedback auxiliary signals was presented. Nonlinear feedback auxiliary signals have several important

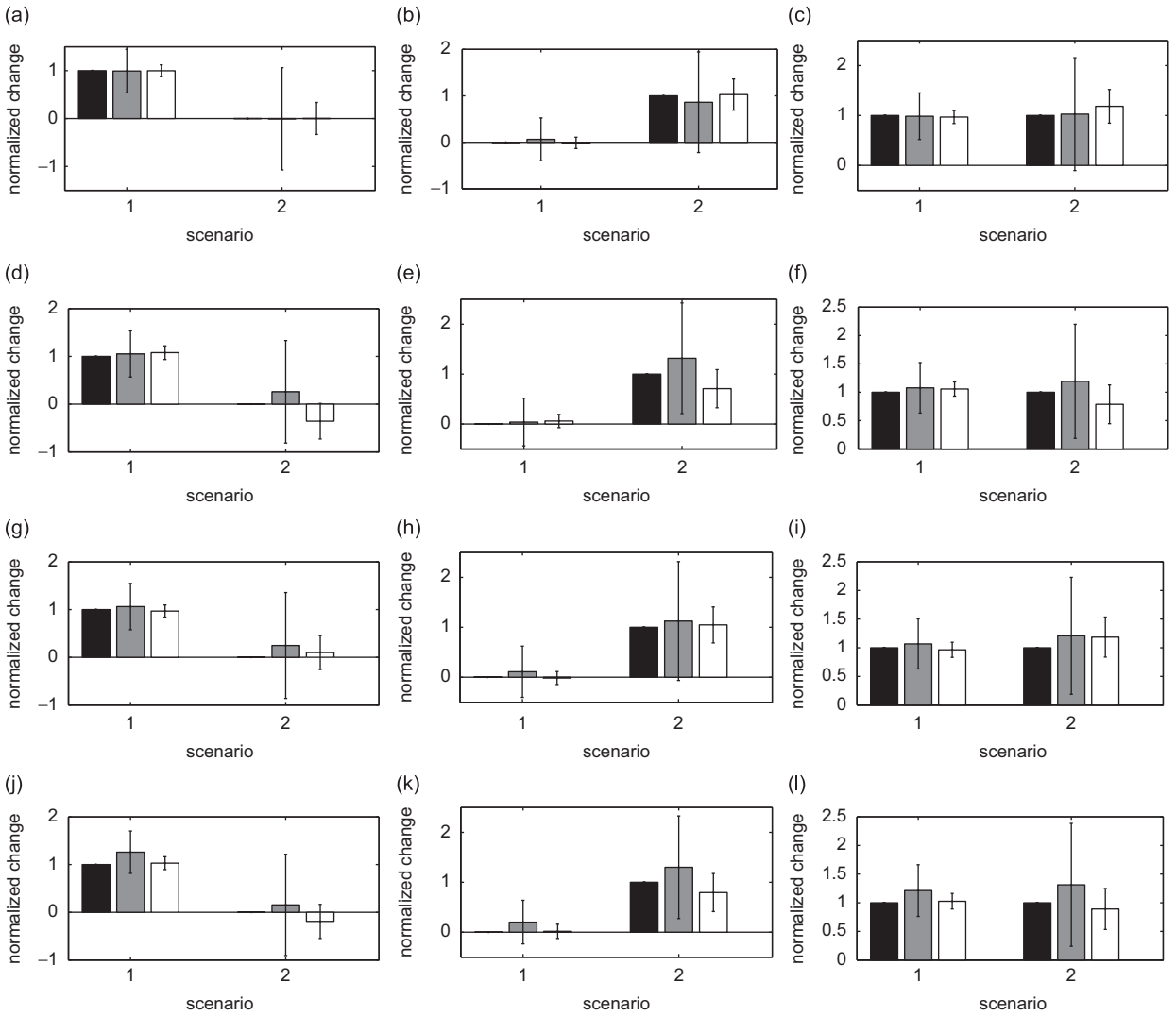

Fig. 6. Sensed mass: (i) by the open loop system (grey), (ii) by a closed loop system designed to be *insensitive* to uniform mass and stiffness changes using *one set* of nonlinear feedback auxiliary signals (white), and (iii) the exact changes (black). Scenario 1 represents changes in mass at the tip. Scenario 2 represents changes in mass at the midspan. (a) Scenario 1, (b) Scenario 2, (c) Scenarios 1 and 2, (d) Scenario 1 with uniform change in mass, (e) Scenario 2 with uniform change in mass, (f) Scenarios 1 and 2 with uniform change in mass, (g) Scenario 1 with uniform change in stiffness, (h) Scenario 2 with uniform change in stiffness, (i) Scenarios 1 and 2 with uniform change in stiffness, (j) Scenario 1 with uniform change in mass and stiffness, (k) Scenario 2 with uniform change in mass and stiffness, and (l) Scenarios 1 and 2 with uniform change in mass and stiffness.

advantages over sensitivity enhancement via traditional linear feedback. These advantages include the complete control over the augmented degrees of freedom with no actuator (physical) effort. Also, augmented variables provide additional sensor knowledge for the augmented degrees of freedom. Additionally, the augmented (fictitious) system does not need to be stable, rather only the physical linearized system needs to be stable.

A difficulty of both traditional feedback and nonlinear feedback auxiliary signals is the need for using active control with the system. Hence, the ability to provide sensitivity enhancement with a reduced number of actuators and sensors is very important. This work demonstrates this ability, and shows the promise of the proposed nonlinear method for use in smart structures. In particular, two systems were explored. The first system contains just one actuator and five sensors and demonstrates the effectiveness of the approach over linear feedback and an uncontrolled system. The additional sensor and control from the augmentation was shown to increase the number of parameters that can be detected. In the second system, a single actuator and just two sensors were used for sensitivity enhancement. In this case, traditional linear feedback methods are not useful in identifying multiple simultaneous parameter variations. However, nonlinear feedback auxiliary signals were shown to detect several simultaneous parameter variations by capitalizing on a special feature of nonlinear feedback auxiliary signals. This feature enables the use of multiple sets of nonlinear feedback auxiliary signals to yield independent augmented frequency information for the same controller configurations.

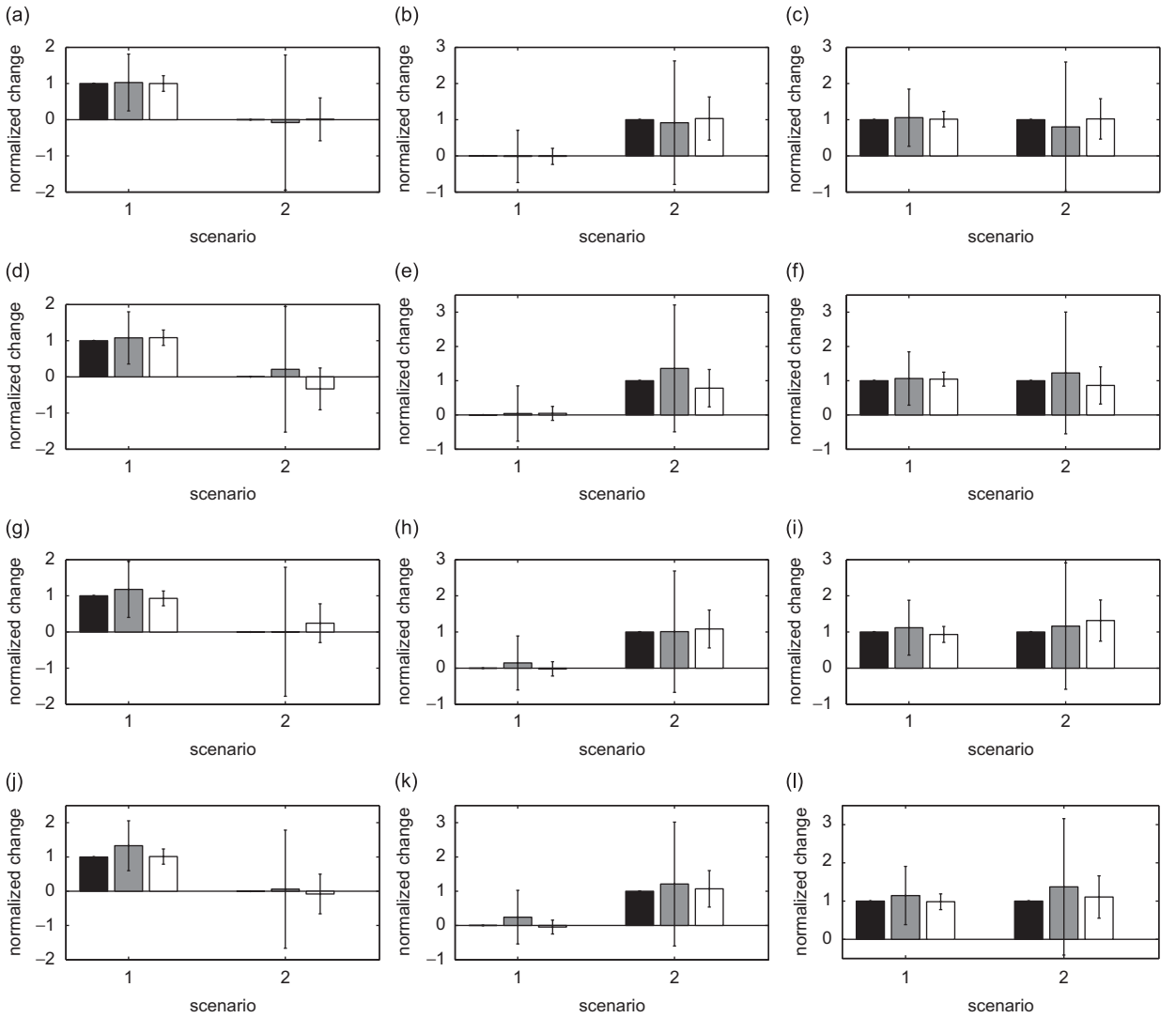

Fig. 7. Sensed mass: (i) by the open loop system (grey), (ii) by a closed loop system designed to be *insensitive* to uniform mass and stiffness changes using *two sets* of nonlinear feedback auxiliary signals (white), and (iii) the exact changes (black). Scenario 1 represents changes in mass at the tip. Scenario 2 represents changes in mass at the midspan. (a) Scenario 1, (b) Scenario 2, (c) Scenarios 1 and 2, (d) Scenario 1 with uniform change in mass, (e) Scenario 2 with uniform change in mass, (f) Scenarios 1 and 2 with uniform change in mass, (g) Scenario 1 with uniform change in stiffness (h) Scenario 2 with uniform change in stiffness, (i) Scenarios 1 and 2 with uniform change in stiffness, (j) Scenario 1 with uniform change in mass and stiffness, (k) Scenario 2 with uniform change in mass and stiffness, (l) Scenarios 1 and 2 with uniform change in mass and stiffness.

In this work, there were several extensions to the method beyond using nonlinear feedback auxiliary signals with a reduced number of actuators and sensors. First, the work detailed a methodology for augmented frequency extraction using noisy and limited measurement data. Also, the work explores the detection of changes in local and global parameters. The local parameters in this case were added masses at the tip and midspan, which corresponded to sensing scenarios. However, if damage detection was the application, the local changes could just as well be stiffness changes. The global changes corresponded to uniform changes in mass and stiffness. These global changes can correspond to certain environmental (temperature or humidity fluctuations) or operational conditions that the user wants to detect. Additionally, an approach to desensitize the resonant frequencies to certain parameters (in this case the global parameters) and increase the sensitivity to other parameters (the local parameters) was introduced. This might prove especially useful in a sensing scenario where the goal is just to detect the mass(es) on a beam, while the environmental or operational conditions are not of interest.

The method was shown to be able to detect very small masses (in the case studied of the order of 0.1 percent of the mass of the physical beam) simultaneously with uniform changes in mass and stiffness with limited physical sensing and actuation. Also, it was shown to be able to detect masses of the same size, while being insensitive to uniform mass and stiffness changes. Numerical simulations were conducted with limited measurements and noisy data.

The present work addresses some of the key challenges in sensitivity enhancing approaches by reducing the number of sensors and amount of control authority needed while still tailoring the dynamics to increase the sensitivity of the resonant frequencies. Although the detection method does not require a model, the optimization algorithm does require at least an approximate model of the system.

Acknowledgment

The authors wish to acknowledge the National Science Foundation for the generous support of this work.

References

[1] K. Wolf, O. Gottlieb, Nonlinear dynamics of a noncontacting atomic force microscope cantilever actuated by a piezoelectric layer, *Journal of Applied Physics* 91 (2002) 4701–4709.
[2] D. DeVoe, Piezoelectric thin film micromechanical beam resonators, *Sensors and Actuators* A 88 (2001) 263–272.
[3] B. Ilic, D. Czaplewski, M. Zalalutdinov, H.G. Craighead, P. Neuzil, C. Campagnolo, C. Batt, Single cell detection with micromechanical oscillators, *Journal of Vacuum Science and Technology* 19 (2001) 2825–2828.
[4] T. Thundat, E.A. Wachter, S.L. Sharp, R.L. Warmack, Detection of mercury-vapor using resonating microcantilevers, *Applied Physics Letters* 66 (1995).
[5] G.Y. Chen, T. Thundat, E.A. Wachter, R.J. Warmack, Adsorption-induced surface stress and its effects on resonance frequency of microcantilevers, *Journal of Applied Physics* 77 (1995).
[6] S.W. Doebling, C.R. Farrar, M.B. Prime, D.W. Shevitz, Damage identification and health monitoring of structural and mechanical systems from changes in their vibration characteristics: a literature review, Los Alamos National Laboratory Report LA-13070-MS, Los Alamos, NM, 1996.
[7] S.W. Doebling, C.R. Farrar, M.B. Prime, A summary review of vibration-based damage identification methods, *Shock and Vibration Digest* 30 (1998) 91–105.
[8] P. Cornwell, M. Kan, B. Carlson, L.B. Hoerst, S.W. Doebling, C.R. Farrar, Comparative study of vibration-based damage identfication algorithms. *Proceedings of the 16th International Modal Analysis Conference*, Part 2. Santa Barbara, CA, 1998, pp. 1710–1716.
[9] M.I. Friswell, J. Penny, The practical limits of damage detection and location using vibration data, *Proceedings of the 11th VPI & SU Symposium on Structural Dynamics and Control*, Blacksburg, VA, 1997, pp. 31–40.
[10] O.S. Salawu, Detection of structural damage through changes in frequency: a review, *Engineering Structures* 19 (1997) 718–723.
[11] N. Stubbs, R. Osegueda, Global non-destructive damage evaluation in solids, *Modal Analysis: The International Journal of Analytical and Experimental Modal Analysis* 5 (1990) 67–79.
[12] N. Stubbs, R. Osegueda, Global damage detection in solids-experimental verification, *Modal Analysis: The International Journal of Analytical and Experimental Modal Analysis* 5 (1990) 81–97.
[13] P.D. Cha, W.T. Gu, Model updating using an incomplete set of experimental modes, *Journal of Sound and Vibration* 233 (2000) 587–600.
[14] N.G. Nalitolela, J.E.T. Penny, M.I. Friswell, Mass or stiffness addition technique for structural parameter updating, *Modal Analysis: The International Journal of Analytical and Experimental Modal Analysis* 7 (1992) 157–168.
[15] J.S. Lew, J.N. Juang, Structural damage detection using virtual passive controllers, *Journal of Guidance, Control, and Dynamics* 25 (2002) 419–424.
[16] L.J. Jiang, J. Tang, K.W. Wang, On the tuning of piezoelectric transducer circuitry network for structural damage identification, *Journal of Sound and Vibration* 309 (2008) 695–717.
[17] A.S.J. Swamidas, Y. Chen, Monitoring crack growth through change of modal parameters, *Journal Sound and Vibration* 186 (1995) 325–343.
[18] R.D. Adams, P. Cawley, C.J. Pye, B.J. Stone, A vibrational technique for non-destructively assessing the integrity of structures, *Journal of Mechanical Engineering Science* 20 (1978) 93–100.
[19] L.R. Ray, L. Tian, Damage detection in smart structures using sensitivity enhancing feedback control, *Journal of Sound and Vibration* 227 (1999) 987–1002.
[20] L.R. Ray, B.H. Koh, L. Tian, Damage detection and vibration control in smart plates: towards multifunctional smart structures, *Journal of Intelligent Material Systems and Structures* 11 (2000) 725–739.
[21] L.R. Ray, S. Marini, Optimization of control laws for damage detection in smart structures, *SPIE Symposium on Mathematics and Control in Smart Structures*, Newport Beach, CA, March 2000, pp. 395–402.
[22] J.N. Juang, K.B. Lim, J.L. Junkins, Robust eigensystem assignment for flexible structures, *Journal of Guidance, Control, and Dynamics* 12 (1989) 381–387.
[23] B.H. Koh, L.R. Ray, Feedback controller design for sensitivity-based damage localization, *Journal of Sound and Vibration* 273 (2004) 317–335.
[24] B.H. Koh, The influence of enhanced closed-loop sensitivity towards breathing-type structural damage, *Journal of Mechanical Science and Technology* 21 (2007) 997–1007.
[25] Z. Wang, F.T.K. Au, Y.S. Cheng, Statistical damage detection based on frequencies of sensitivity-enhanced structures, *International Journal of Structural Stability and Dynamics* 8 (2008) 231–255.
[26] L.J. Jiang, J. Tang, K.W. Wang, An optimal sensitivity-enhancing feedback control approach via eigenstructure assignment for structural damage identification, *ASME Journal of Vibration and Acoustics* 129 (2007) 771–783.
[27] L.J. Jiang, K.W. Wang, An experiment-based frequency sensitivity enhancing control approach for structural damage detection, *Smart Materials and Structures* 18 (2009) 1–12.
[28] K. D'Souza, B.I. Epureanu, Damage detection in nonlinear systems using optimal feedback auxiliary signals. *ASME Journal of Vibration and Acoustics* 132 (2010), doi:10.1115/1.4000839.
[29] K. D'Souza, B.I. Epureanu, Nonlinear feedback auxiliary signals for system interrogation and damage detection, *Philosophical Transactions of the Royal Society of London: A—Mathematical, Physical and Engineering Sciences* 464 (2008) 3129–3148.
[30] K. D'Souza, B.I. Epureanu, Damage detection in nonlinear systems using system augmentation and generalized minimum rank perturbation theory, *Smart Materials and Structures* 14 (2005) 989–1000.
[31] K. D'Souza, B.I. Epureanu, Multiple augmentations of nonlinear systems and generalized minimum rank perturbations for damage detection, *Journal of Sound and Vibration* 316 (2008) 101–121.
[32] K. D'Souza, B.I. Epureanu, Sensor placement for damage detection in nonlinear systems using system augmentations, *AIAA Journal* 46 (2008) 2434–2442.
[33] J. Leuridan, Some Direct Parameter Model Identification Methods Applicable For Multiple Modal Analysis, Ph.D. Thesis, Department of Mechanical and Industrial Engineering, University of Cincinnati, 1984.
[34] T. Coleman, M.A. Branch, A. Grace, Opimization Toolbox User's Guide, The MathWorks, Inc., 1999.